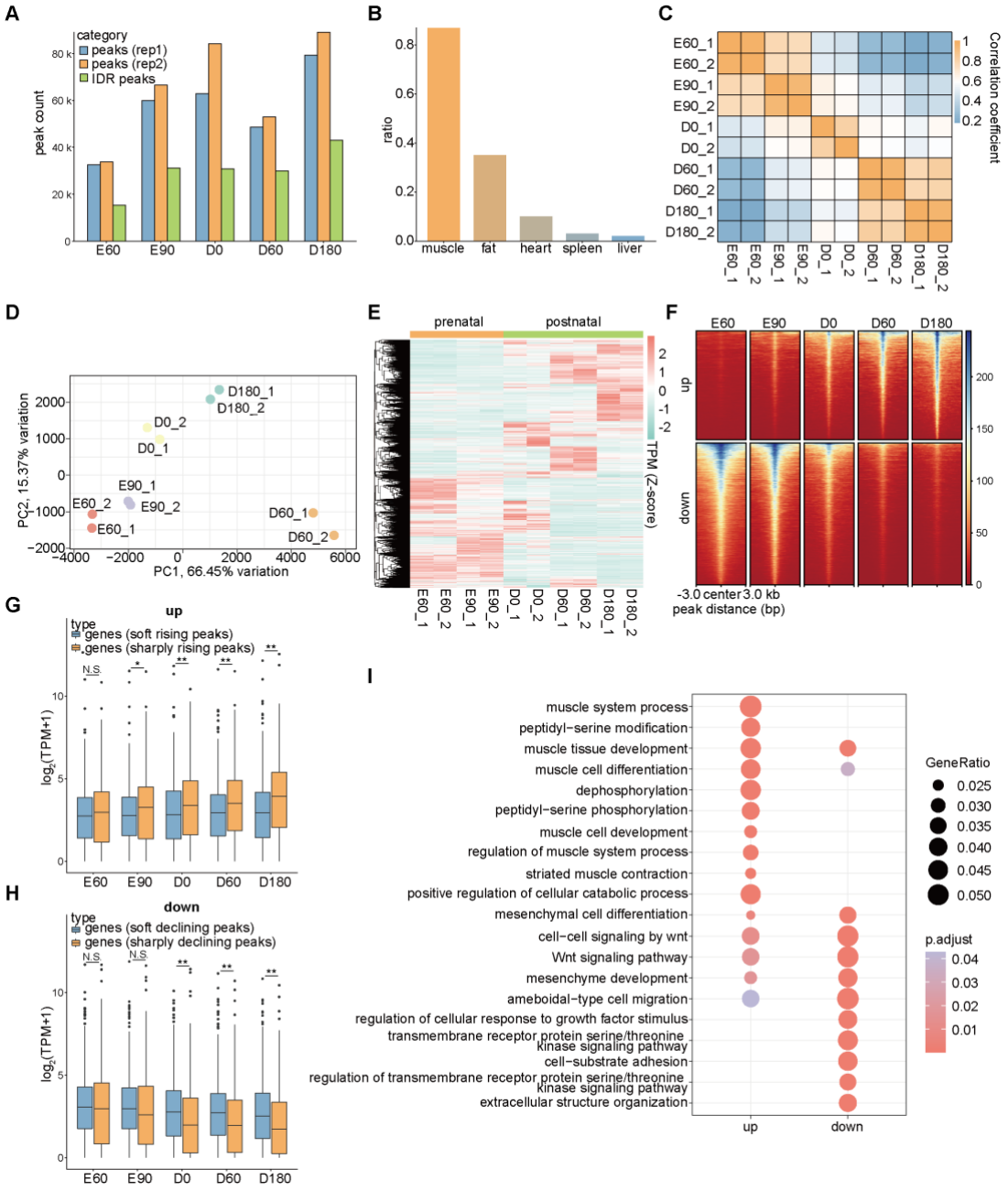

Supplemental Figure S1. Overview of CUT&Tag H3K27ac peaks. (*A*) Number of H3K27ac peaks per developmental stage (1k represents 1000). Two biological replicates were included at each stage. Peaks were independently called for each replicate, and the peak sets were merged using IDR method to generate a non-redundant and robust peak set (IDR peaks) with optimal intra-group consistency. (*B*) Proportion of tissue-specific enhancers in pigs that intersected with the H3K27ac peaks identified in this study. These enhancers were extracted from the study conducted by Zhao Y

et al. (PMID: 33850120). (*C*) Sample similarity clustering based on pairwise Pearson correlations calculated from the IDR peak signal matrix. (*D*) Principal component analysis of PSM samples based on H3K27ac peaks. (*E*) Hierarchical clustering of H3K27ac peaks across PSM samples. (*F*) Heatmap depicting the signals of up- and down-regulated peaks. Continuously up- and down-regulated peaks were identified using STEM software and visualized with deepTools. (*G*-*H*) Expression changes of genes associated with up- (*G*) and down-regulated (*H*) peaks (see Methods for details on peak-associated gene identification). The normalization method for read counts is Transcripts Per Million (TPM). (*I*) GO enrichment analysis of up- and down-regulated H3K27ac peaks.

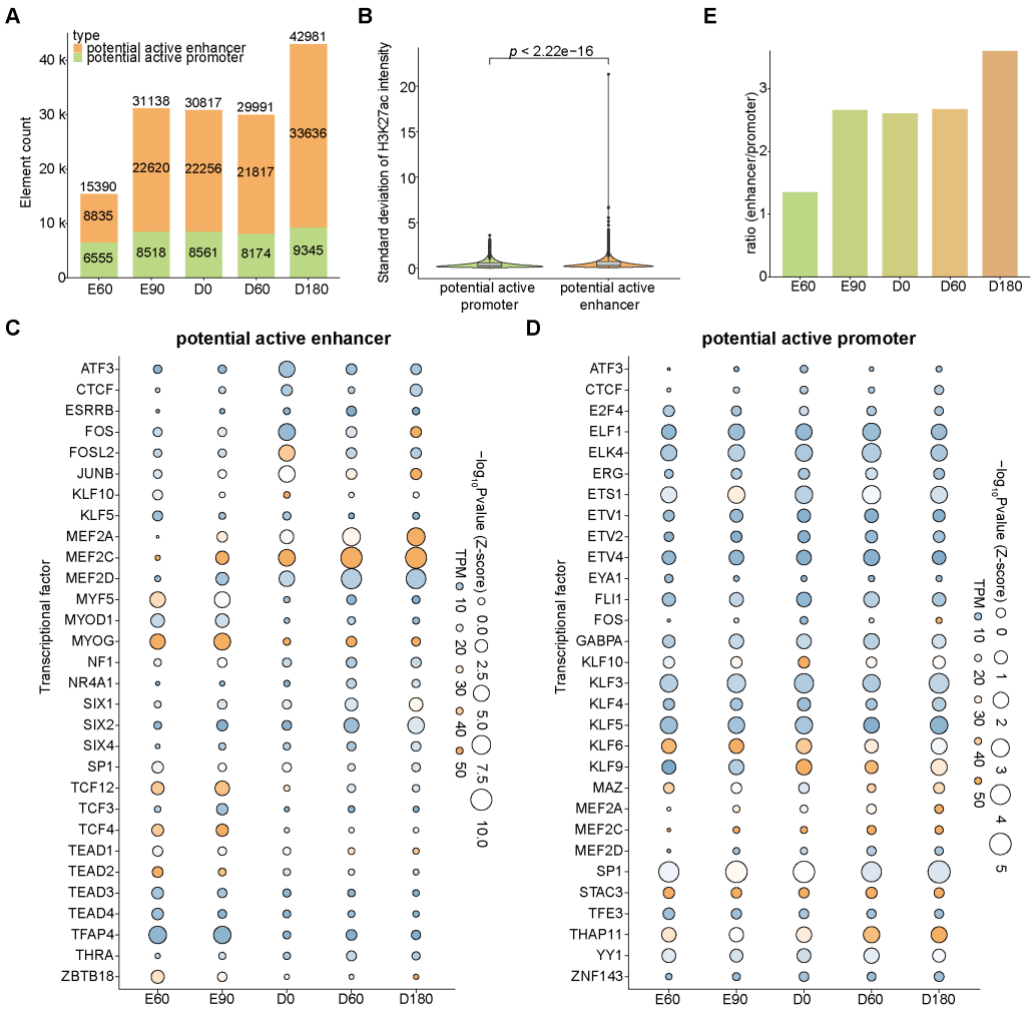

Supplemental Figure S2. Partitioning promoters and enhancers from H3K27ac peaks. (*A*) Number of potential active promoters and enhancers at each developmental stage. Proximal H3K27ac peaks from TSSs were identified as potential active promoters, while distal H3K27ac peaks were identified as potential active enhancers. (*B*) Comparison of signal dynamics at promoters and enhancers during development. The intensity of H3K27ac was standardized using a Z-score. (*C-D*) Top 30 TF motifs with the highest standard deviation of significance *p*-value in enhancers (*C*) and promoters (*D*) across five developmental stages. Only TFs with significant motif enrichment (*p*-value < 1e-10 at least at one stage) and sufficient mRNA abundance (TPM ⩾ 3 at least at one stage) were retained. (*E*) Ratio of enhancers to promoters at each stage.

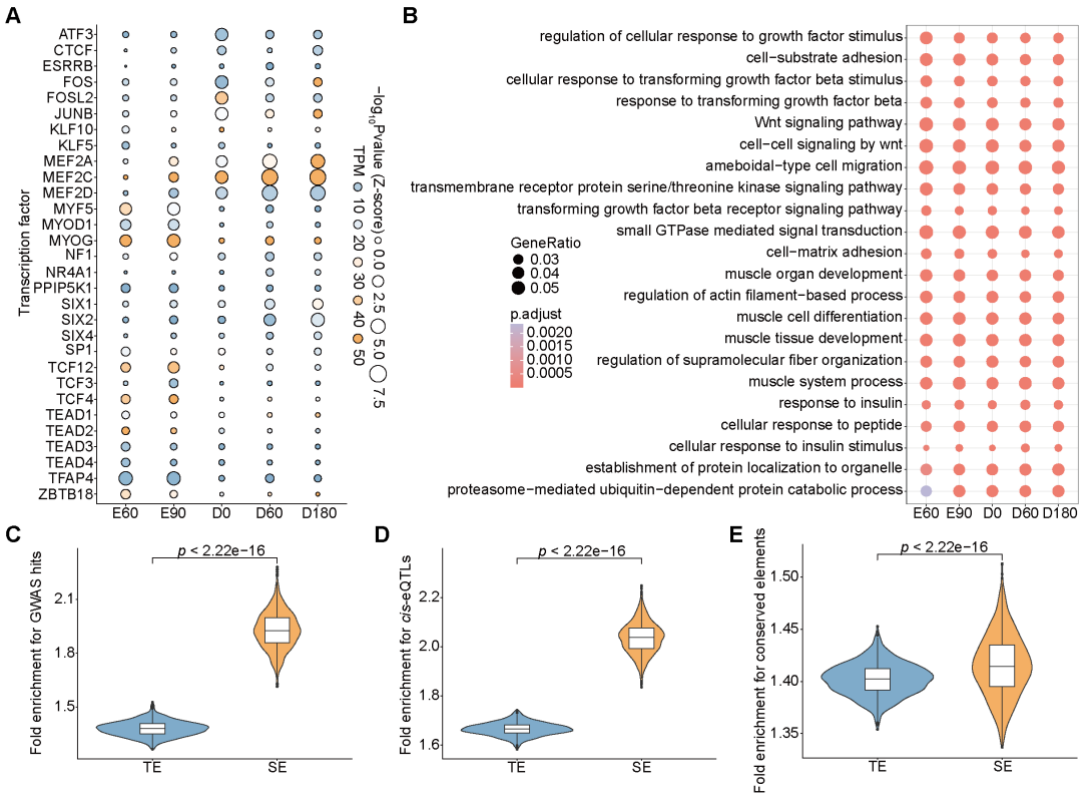

Supplemental Figure S3. Characteristics of TEs and comparison with SEs. (*A*) Top 30 TF motifs exhibiting the greatest standard deviation of significance *p*-values in TEs across five developmental stages. Only TFs with significant motif enrichment (*p*-value < 1e-10 at least at one stage) and sufficient mRNA abundance (TPM ⩾ 3 at least at one stage) were retained. (*B*) GO enrichment analysis of TEs at each stage. (*C*) Fold enrichment of SEs and TEs for GWAS hits associated with pig meat and carcass traits from the Animal QTLdb. (*D*) Fold enrichment of SEs and TEs for porcine skeletal muscle *cis*-eQTLs from the PigGTEx portal. (*E*) Fold enrichment of SEs and TEs for mammalian conserved DNA elements based on Genomic Evolutionary Rate Profiling (GERP).

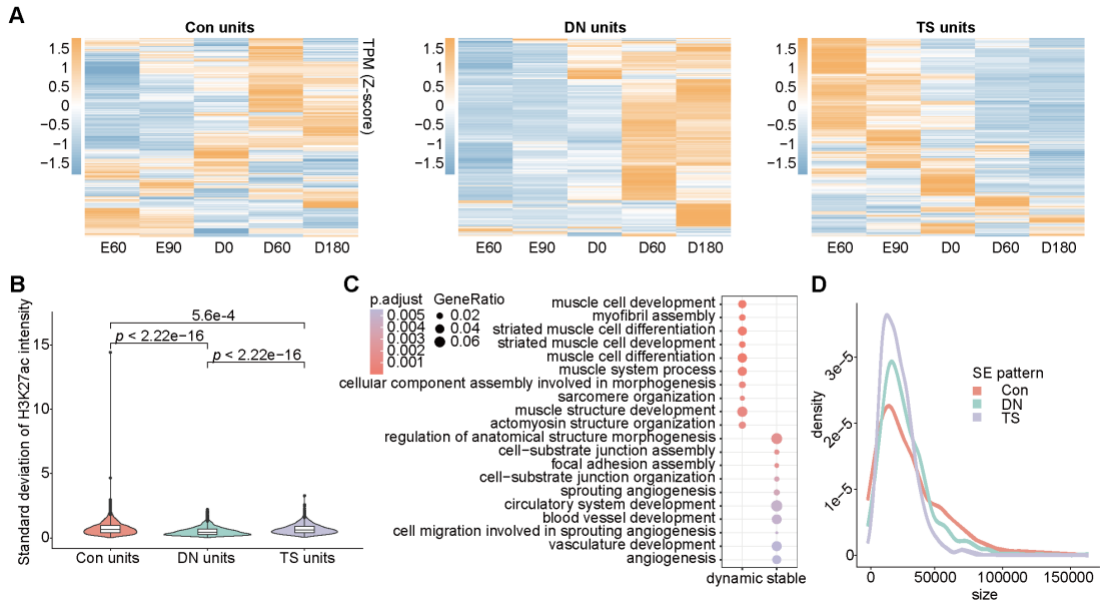

Supplemental Figure S4. Distinct temporal SEs. (*A*) Heatmap presenting H3K27ac read intensities of constituent enhancer units in the three classes of SEs. (*B*) Comparative analysis of the signal dynamics of constituent enhancer units in the three types of SEs. Z-score normalized H3K27ac intensity was used to calculate the standard deviation, with a higher standard deviation indicating greater dynamism. (*C*) GO enrichment analysis of dynamic and stable peaks across the five developmental stages of PSM. Based on the magnitude of signal variance (standard deviation), the first 5000 peaks are defined as dynamic peaks, while the last 5000 peaks are defined as stable peaks. (*D*) Size distribution of three types of temporal SEs. Despite the size differences, we ensured that the enrichment analysis of these SE types for genome annotations was not affected by SE size. This was achieved by using simulated Con, DN, and TS SEs based on their size distributions to account for the size distribution differences.

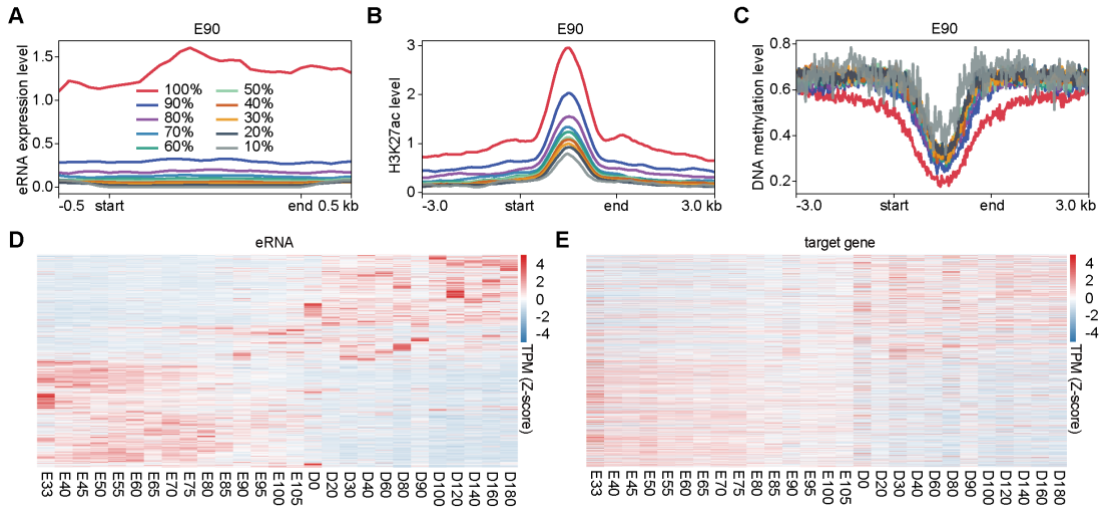

Supplemental Figure S5. Association between eRNA signals and other omics signals. (*A-C*) Correspondence among eRNA expression levels (*A*), H3K27ac intensity (*B*), and DNA methylation levels (*C*) at E90 stage. Expressed eRNAs were equally divided into 10 groups from low expression (10%) to high (100%) based on their abundance. Mean-normalized RNA-seq density, CUT&Tag density or WGBS DNA methylation levels were plotted within eRNA bodies and their flanking regions for each group of eRNAs. **(***D-E***)** Heatmaps depicting expression levels of eRNAs (*D*) and their corresponding predicted target genes (*E*) across 27 PSM development stages.

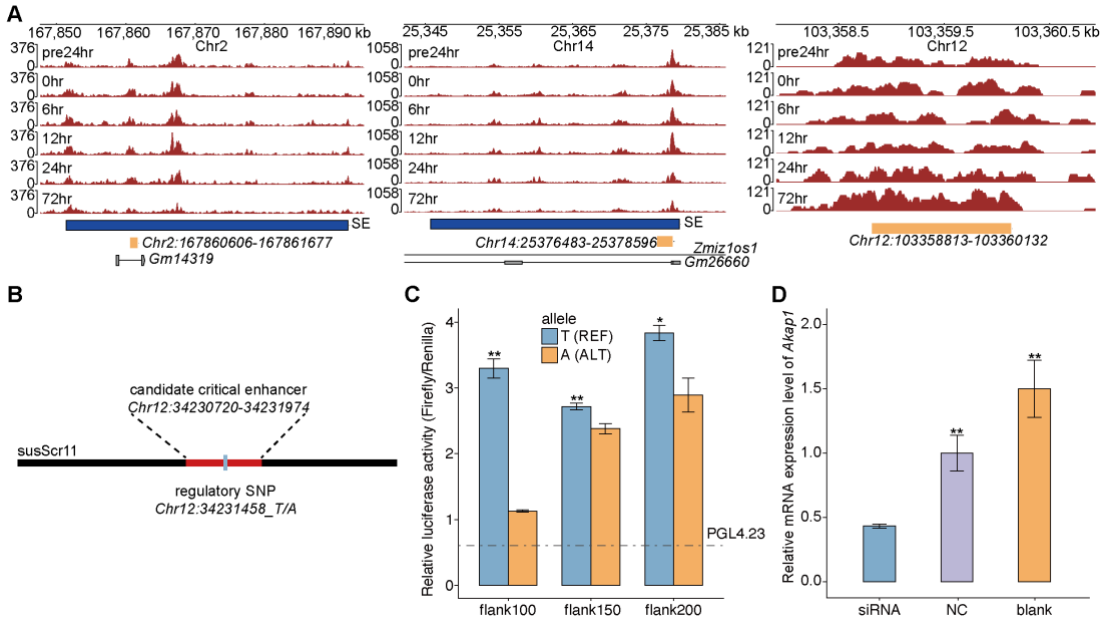

Supplemental Figure S6. Evidence supporting the regulatory function of candidate critical enhancers. (*A*) Genome browser snapshots displaying mouse orthologous sequences for three candidate critical enhancers with Con SEs. The tracks depicted represent H3K27ac ChIP-Seq signals across 6 stages during C2C12 myogenesis. The 24 hours prior to induction of differentiation are denoted by "pre24hr," and so forth. (*B*) Luciferase reporter assay of a regulatory SNP. The candidate critical enhancer *Chr12:34230720-34231974* harboring the regulatory SNP *Chr12_34231458_T_A* in the pig genome. (*C*) The impact of reference (REF) and alternate (ALT) alleles of the SNP on enhancer activity was assessed using a luciferase reporter assay. The term "flank100" denotes the genomic region of 100 base pairs centered on the SNP, and so forth. (*D*) Interference of the predicted target gene *Akap1* by siRNA. qPCR assays demonstrate the siRNA-mediated knockdown of *Akap1* in C2C12 cells at myogenic differentiation day 7, compared to blank and NC groups.

Supplemental Figure S7. Sequence deletion mediated by CRISPR-Cas9 pgRNAs in C2C12 cells. The deleted sequence corresponds to the mouse orthologous sequence of the candidate critical enhancer *Chr12:34230720-34231974*. The upper section labels the locations of the deleted sequence, gRNAs, cleavage sites, and PCR primers. The lower section presents the sequencing results of PCR products with annotated cleavage sites.

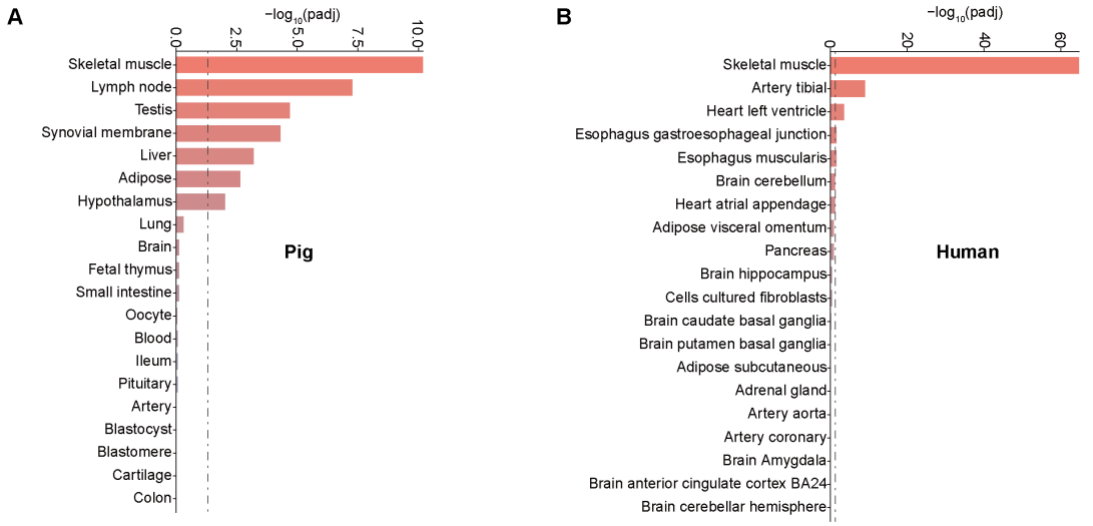

Supplemental Figure S8. Skeletal muscle-specific *cis*-eQTL enrichment. (*A*) Enrichment of skeletal muscle-specific enhancers in pig tissue-specific *cis*-eQTLs from the PigGTEx portal. Skeletal muscle-specific enhancers were generated by excluding enhancers from non-skeletal muscle tissues in pigs from our potential active enhancers. (*B*) Enrichment of human skeletal muscle-specific enhancers in human tissue-specific *cis*-eQTLs from the GTEx portal. Using the same method, enhancers from human tissues in ENCODE were processed to produce human skeletal muscle-specific enhancers. Enrichment significance was calculated using hypergeometric testing, with FDR correction applied for multiple comparisons.